Hindawi
Geofluids
Volume 2017, Article ID 9745795, 16 pages
https://doi.org/10.1155/2017/9745795

Research Article

Gas-Water Flow Behavior in Water-Bearing Tight Gas Reservoirs

Renyi Cao,[1] Liyou Ye,[2] Qihong Lei,[3] Xinhua Chen,[1] Y. Zee Ma,[4] and Xiao Huang[1]

[1]*School of Petroleum Engineering, China University of Petroleum, Beijing 102249, China*
[2]*Department of Porous Flow & Fluid Mechanics, PetroChina RIPED, Langfang 065007, China*
[3]*Research Institute of Exploration and Development, Changqing Oil Field, PetroChina, Shaanxi 710021, China*
[4]*Schlumberger, Denver, CO 80202, USA*

Correspondence should be addressed to Renyi Cao; caorenyi@126.com

Received 6 March 2017; Accepted 31 July 2017; Published 27 September 2017

Academic Editor: Shuyu Sun

Some tight sandstone gas reservoirs contain mobile water, and the mobile water generally has a significant impact on the gas flowing in tight pores. The flow behavior of gas and water in tight pores is different than in conventional formations, yet there is a lack of adequate models to predict the gas production and describe the gas-water flow behaviors in water-bearing tight gas reservoirs. Based on the experimental results, this paper presents mathematical models to describe flow behaviors of gas and water in tight gas formations; the threshold pressure gradient, stress sensitivity, and relative permeability are all considered in our models. A numerical simulator using these models has been developed to improve the flow simulation accuracy for water-bearing tight gas reservoirs. The results show that the effect of stress sensitivity becomes larger as water saturation increases, leading to a fast decline of gas production; in addition, the nonlinear flow of gas phase is aggravated with the increase of water saturation and the decrease of permeability. The gas recovery decreases when the threshold pressure gradient (TPG) and stress sensitivity are taken into account. Therefore, a reasonable drawdown pressure should be set to minimize the damage of nonlinear factors to gas recovery.

1. Introduction

Water-bearing tight gas reservoirs, as part of unconventional reservoirs, attract more and more attention. In comparison with non-water-bearing tight gas reservoirs, the gas recovery of water-bearing tight gas reservoirs is generally lower, and three factors strongly influence the development of water-bearing gas reservoirs and flow behavior. The first influencing factor is the threshold pressure gradient (TPG) due to mobile water and small pore-throat, which needs to be overcome for initiating flow. The second influencing factor is the stress sensitivity of the permeability, which is common for tight gas reservoirs but intensified by water existence. The third influencing factor is the gas-water relative permeability, which is impacted by the variation of drawdown pressure. These three factors may act together and affect the gas flow and production of tight gas reservoirs. Accurate description and reasonable characterization of nonlinear features of gas flow are the foundation for predicting gas production.

The theories and models regarding the effect of TPG on water-oil two-phase flow have been proposed [1–6], and experiments were conducted to study the pseudo-TPG and analyze the reason for which the pseudo-TPG has to be overcome for flow in ultra-low permeability tight reservoirs [3, 7, 8]. However, less attention has been paid to the effect of water saturation on TPG of gas phase, especially for water-bearing tight gas reservoirs. Water saturation influences the gas flow by changing the gas slip factor. The gas slip factor will decrease with the increase of water saturation [9]. Ding et al. [10] conducted experimental studies about the dynamic threshold pressure in a water-bearing tight gas reservoir and found that TPG varied with the change of pore pressure and water saturation. Cores with a higher water saturation had a higher TPG than cores with a lower water saturation, and the TPG showed higher-amplitude change as well (TPG sensitivity coefficient is bigger). The question is, how will permeability and water saturation simultaneously affect the TPG of water-bearing tight gas reservoirs?

Stress sensitivity of formation has been quite extensively studied. In one of the earliest studies of permeability sensitivity to the stress, Fatt and Davis [11] found that the magnitude of the formation permeability reduction ranged from 11% to 41%. Confining pressure acting on the rock core has a very important impact on the magnitude of permeability. Thomas and Ward [12] found that gas permeability of tight sandstone formations would be markedly reduced with increasing overburden pressure. Permeability reduction of cores due to stress in other formations was also studied by other authors [13–15]. A comprehensive study on micro-pore-throat structure and pore-throat distribution of tight reservoir rock using SEM and constant-rate mercury injection technology was also reported (Yu et al. [16]). Quantitatively, Jones and Owens [17] proposed a coefficient to describe permeability stress sensitivity as follows:

$$s_J = \frac{\left\{1 - \left[K_g\left(\sigma_{\text{eff}}\right)/K_g\left(\sigma_{\text{eff}} = 6.89\right)\right]^{1/3}\right\}}{\lg\left(\sigma_{\text{eff}}/6.89\right)}. \quad (1)$$

Luo et al. [18] conducted experiments using gas to analyze stress sensitivity. The Klinkenberg permeability of cores used in the experiments ranges from 0.1 mD to 3 mD. Based on the experiments, they derived the following equation (or coefficient) to characterize the stress sensitivity:

$$s_L = \frac{-\lg\left(K_{g\,\min}/K_{\text{go}}\right)}{\lg\left(\sigma_{\text{eff max}}/\sigma_{\text{effo}}\right)}. \quad (2)$$

These studies all imply that rock permeability reduction due to the increase of effective stress could significantly affect oil well productivity, especially for tight formations. However, there is still little research on the stress sensitivity of water-bearing tight gas reservoir. Water is the wetting phase for most formations. There is a water film attached on the inner surface of pores. Though the water film is thin, it has a significant impact on the flow (normally in micro- or nanometer scale) of tight gas reservoirs. The thickness of the water film is a function of pore pressure, and thus it is stress sensitivity. Once the stress changes, the flow channel will vary due to the changing boundary layer. Correspondingly, the flow capacity of formation will make a difference. Yet, whether the magnitude of water saturation will affect the stress sensitivity remains unknown.

Relative permeability plays an essential role for reservoir simulation and production prediction. A number of studies have been published on the relative permeability of different types of formations. Burdine [19] investigated the relative permeability using pore size distribution data. Corey [20] presented a method of calculating relative permeability with exponential coefficients based on the empirical understanding. Fatt [21] simulated the overburden pressure and investigated gas-oil relative permeability under different overburden pressures. Al-Quraishi and Khairy [22] investigated the effect of pore pressure variation on the oil-water relative permeability curves at fixed overburden pressures and the effect of confining pressure on the relative permeability curves at constant pore pressure. However, reports on the effect of the drawdown pressure on the relative permeability are less common. According to Gao et al. [23], the drawdown pressure gradient significantly affects the gas-water relative permeability, and the relative permeability curve moves to the right as the drawdown pressure gradient increases; however, the mechanism of the relationship between the drawdown pressure gradient and the gas-water relative permeability was not discussed in that article. Mo et al. [24] investigated the effect of the drawdown pressure on the relative permeability of tight gas reservoirs and showed that the displacement pressure had a significant effect on the relative permeability.

Three factors strongly influence the development of the water-bearing gas reservoir and flow behavior. The first factor is the TPG due to mobile water and small pore-throats, which needs to be overcome for initiating flow. The second factor is the stress sensitivity of the gas permeability, which is common for a tight gas reservoir but intensified by presence of water. The third factor is the gas-water relative permeability, which changes with variation of drawdown pressure. These three factors work simultaneously and affect the gas flow and production of tight gas reservoirs. Accurate description and characterization of nonlinearity of gas flow are fundamental for predicting gas production.

This article analyzes these three influencing factors of gas recovery and flow behavior of water-bearing gas reservoirs and then presents a gas-water two-phase flow model for tight gas reservoirs while quantifying and analyzing the effect of each nonlinear factor on gas well productivity and recovery. Finally, measurements for enhanced gas recovery of water-bearing tight gas reservoirs are made. This model provides theoretical basis for the development of tight gas reservoir.

2. Flow Behavior and Formation Properties of Water-Bearing Tight Gas Reservoirs

Experimentations of flow behavior and formation properties in tight gas reservoir bearing water [25–27] have shown that water influences stress sensitivity of tight reservoirs and increases threshold pressure gradient. In addition, the capacity of gas-water two-phase percolation is significantly different under different displacement pressure gradient.

2.1. Method of Experiment. We carried out the core displacement experiments by a series of the radius of 2.5-centimeter and the length of 5-centimeter natural cores. And experimental apparatus and experimental process are the same as the conventional core displacement experiments, and the main experiment equipment is core holding unit, circulating pump, pressure sensor, and so forth. Experimental steps include core evacuation, saturated water, saturated gas, and displacement.

We studied the threshold pressure gradient under different water saturation by taking the core saturation to different initial water saturation and then carrying out the displacement experiments and measured the stress sensitivity coefficient under different water saturation to study the relationship between stress sensitivity coefficient and water saturation and permeability; and a series of relative permeability

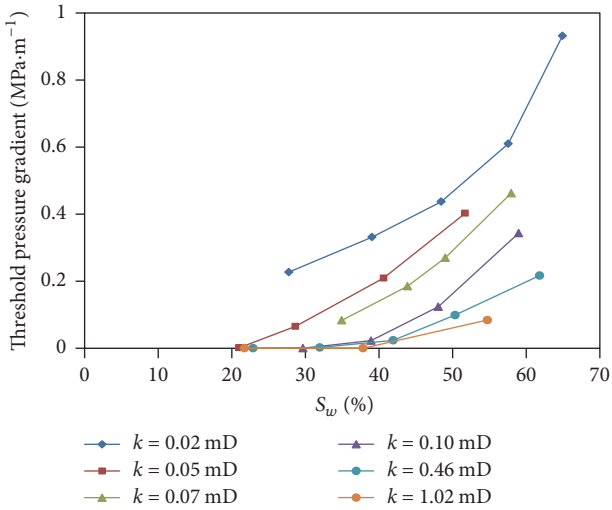

Figure 1: The relationship between water saturation (S_w) and threshold pressure gradient for different permeabilities.

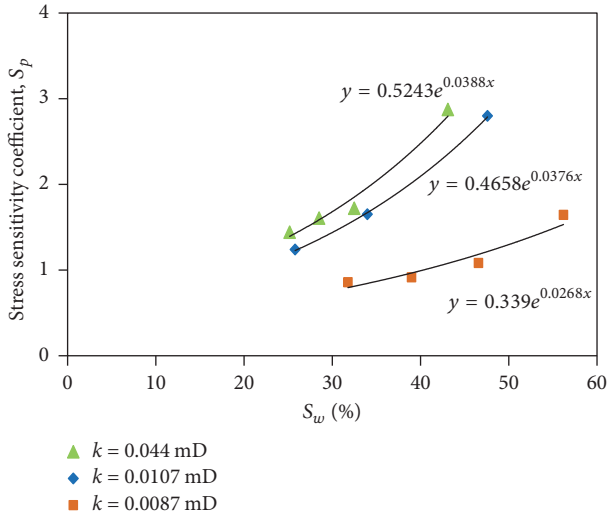

Figure 2: Relationship between water saturation (S_w) and stress sensitivity coefficient.

curves were conducted under different displacement pressure gradient to study the relationship between displacement pressure and relative permeability. For the details and results of experiments, one could refer to the papers by Ye [25, 27], and parts of results were redrawn in Figures 1–3.

2.2. Effect of Threshold Pressure Gradient. For a gas reservoir without mobile water, the gas is continuous phase and gas viscosity is very low, and there is no TPG for single gas phase flowing in tight formations. When the water saturation is higher than irreducible water saturation, the mobile water could impact the gas flow. This is because the water exists in the surface of rock at small throat due to water wettability in tight formation and the gas distributes in pores, and this phenomenon results in mutual interaction between water phase and gas phase. For the water-gas two phases in tight

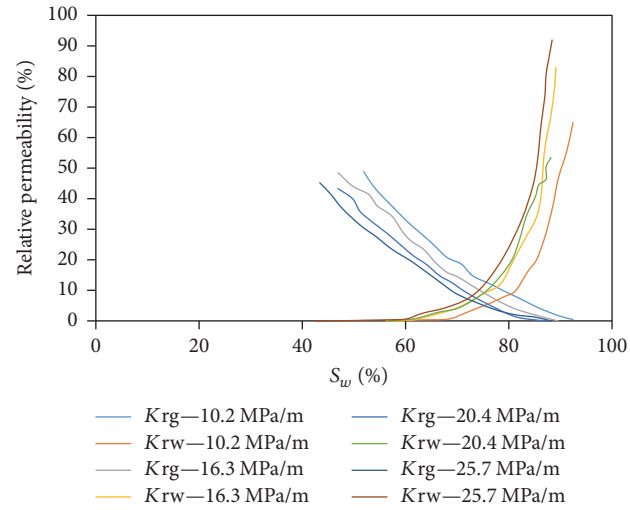

Figure 3: Gas-water relative permeability under different drawdown pressure gradient.

formations, if the gas phase starts flowing, the gas should break the block of water phase in throat and drive the water phase starting to flow, and this process should overcome some extra pressure gradient. As such, the block of water to gas results in TPG, and the motion equation with TPG could be described as follows:

$$v = -\frac{K}{\mu}\left[\nabla p - \lambda\right]. \tag{3}$$

The experiments show that the TPG of gas-water two-phase flow is correlated to water saturation and permeability (Figure 1 and [27]), and the TPG is the function of water saturation and permeability. The fitting equation to the experiment results indicate that when the irreducible water saturation is constant, the TPG and permeability have a power relationship:

$$\lambda = aK^{b(1-S_w)}e^{S_w}, \tag{4}$$

where a and b are fitting coefficients.

2.3. Effect of Stress Sensitivity. When gas flows as a single phase in a tight gas reservoir, stress significantly affects gas well productivity.

$$\frac{K}{K_i} = \left(\frac{\sigma}{\sigma_i}\right)^{-S_p} = \left(\frac{p_c - p}{p_c - p_i}\right)^{-S_p}, \tag{5}$$

where S_p is the factor of stress sensitivity, such as $S_p = cK^{-n}$. This formula is widely used to study effect of stress sensitivity and can be applied to water-bearing gas reservoirs. However, the coefficients in this formula must be refitted when it is applied to various reservoirs.

However, when water is also present in a tight gas reservoir, water not only affects the gas flow, but also has an effect on the stress of the reservoir [28, 29]. Experimental results show that stress is intensified as water saturation

increases (Figure 2 and [27]). It is mainly because the presence of water reduces the flow path of gas. For tight gas reservoirs with larger original water saturation, the stress variation during production will result in a redistribution of water film and thus affects gas permeability, intensifies stress sensitivity, and thus aggravates stress damage. In addition, the physicochemical reactions between water and minerals in tight sandstones reduce the compressive strength of rock and further intensify stress sensitivity. Therefore, water presence will strengthen the stress of tight sandstones.

Stress sensitivity coefficient of water-bearing tight gas reservoirs is

$$S_p = cK^{-n}e^{d\cdot S_w}. \tag{6}$$

2.4. Relative Permeability of Gas-Water Flow. Understanding the relative permeability is important for the prediction of production performance of water-bearing tight gas reservoirs. Compared to the conventional gas reservoirs of low permeability, the relative permeability of gas-water flow in tight formations is more complex because of the extremely small pores and throats. The comparison of gas-water two-phase flow experiments under different pressures shows that displacement pressure gradient impacts the gas-water relative permeability. The experimental results (Figure 3) show that as displacement pressure increases [27], the relative permeability of water increases sharply, while the relative permeability of gas reduces, and the residual gas saturation reduces. Therefore, gas-water relative permeability and the endpoint of saturation are a function of both water saturation and pressure gradient, such as

$$\begin{aligned} K_g &= KK_{\mathrm{rg}}\left(S_w, \nabla p\right) \\ K_w &= KK_{\mathrm{rw}}\left(S_w, \nabla p\right) \\ S_{\mathrm{gr}} &= S_{\mathrm{gr}}\left(\nabla p\right). \end{aligned} \tag{7}$$

3. Model of Gas-Water Flow in Tight Formation

To simplify the gas-water two-phase flow modeling while honoring nonlinear flow behavior, the following assumptions are made in the model construction and percolation simulation:

(1) The simulation process is gas-water two-phase flow with capillary force taken into account.

(2) Gas and water are mutually immiscible and water phase is incompressible.

(3) Stress effect to the formation porosity is neglected.

(4) Fluid flow happens under constant temperature.

(5) Gravity force is ignored.

3.1. Motion Equation. For gas-water two-phase flow in tight gas reservoirs, we take the separate single phase flow conforming to Darcy's law. As for the expression of pressure gradient, TPG has to be deducted from the displacement pressure gradient.

$$\begin{aligned} \overrightarrow{v}_g &= -\frac{K\left(p\right)K_{\mathrm{rg}}}{\mu_g}\left[\mathrm{grad}\left(p_g\right) - \lambda\right] \\ \overrightarrow{v}_w &= -\frac{K\left(p\right)K_{\mathrm{rw}}}{\mu_w}\left[\mathrm{grad}\left(p_w\right) - \lambda\right], \end{aligned} \tag{8}$$

where TPG is expressed in (4).

3.2. Continuity Equation. In gas-water two-phase percolation, the continuity equations are as follows:

Gas phase:

$$\begin{aligned} &-\left(\frac{\partial\left(\rho_g v_{gx}\right)}{\partial x} + \frac{\partial\left(\rho_g v_{gy}\right)}{\partial y} + \frac{\partial\left(\rho_g v_{gz}\right)}{\partial z}\right) + q_g \\ &\quad = \frac{\partial\left(\phi\rho_g S_g\right)}{\partial t}. \end{aligned} \tag{9}$$

Water phase:

$$\begin{aligned} &-\left(\frac{\partial\left(\rho_w v_{wx}\right)}{\partial x} + \frac{\partial\left(\rho_w v_{wy}\right)}{\partial y} + \frac{\partial\left(\rho_w v_{wz}\right)}{\partial z}\right) + q_w \\ &\quad = \frac{\partial\left(\phi\rho_w S_w\right)}{\partial t}. \end{aligned} \tag{10}$$

3.3. Permeability and Stress Relationship

$$K\left(p\right) = K_i\left(\frac{p_c - p}{p_c - p_i}\right)^{-S_p}, \tag{11}$$

where stress sensitivity coefficient is $S_p = cK^{-n}e^{d\cdot S_w}$.

3.4. Model of Relative Permeability of Gas and Water. The relative permeability model could be obtained by interpolating the relative permeability under low (Figure 4(a)) and high (Figure 4(b)) pressure. The relative permeability model is shown in the following equations:

$$\begin{aligned} S_{\mathrm{wD}} &= \frac{S_w - S_{\mathrm{wc}}}{1 - S_{\mathrm{wc}} - \left(1 - S_{\mathrm{gr}}\right)} \\ K_{\mathrm{rw}} &= f \times S_{\mathrm{wD}}^n \\ K_{\mathrm{rg}} &= g \times \left(1 - S_{\mathrm{wD}}\right)^m \\ S_{\mathrm{gr}} &= S_{\mathrm{grh}} + \frac{S_{\mathrm{grl}} - S_{\mathrm{grh}}}{\Delta p_h - \Delta p_l}\left(\Delta p_h - \Delta p_l\right), \end{aligned} \tag{12}$$

where S_{wD} is the dimensionless water saturation; f, g, m, n are the fitting coefficients; Δp_h is the high displacement pressure gradient; Δp_l is the low displacement pressure gradient; S_{grl} is the residual gas saturation corresponding to Δp_l; S_{grh} is the residual gas saturation corresponding to Δp_h.

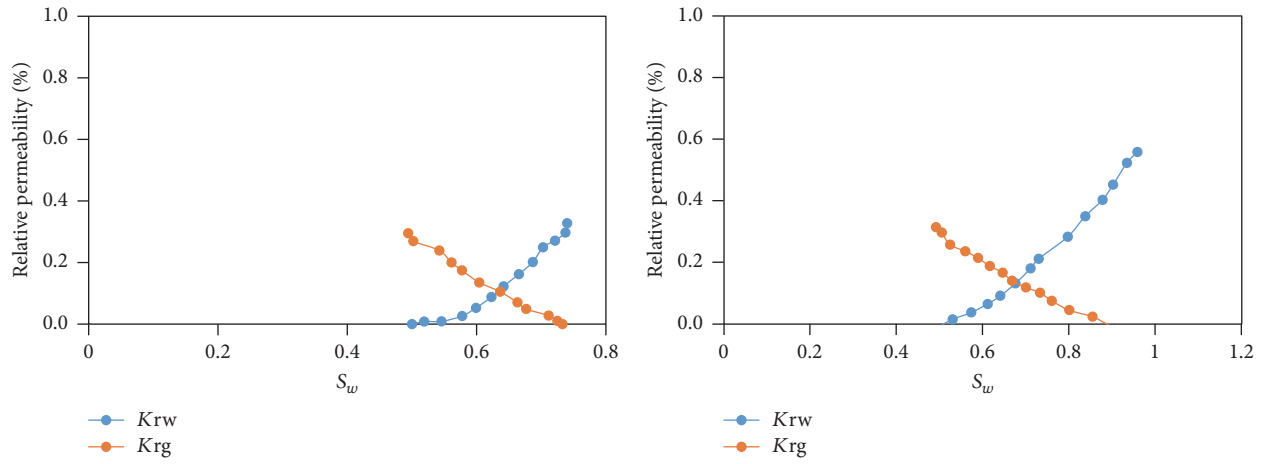

(a) Low drawdown pressure gradient

(b) High drawdown pressure gradient

FIGURE 4: Gas-water relative permeability under different drawdown pressure gradient.

3.5. Fundamental Differential Equation. From all the aforementioned equations together, we can get the fundamental differential equation as follows:

For water phase,

$$\nabla \cdot \left[\frac{K(p) K_{\mathrm{rw}}}{B_w \mu_w} \left(\nabla p_g - \nabla p_{\mathrm{cgw}} - \lambda_w \right) \right] + \frac{q_w}{\rho_{\mathrm{wsc}}} = \frac{\partial}{\partial t} \left(\frac{\phi S_w}{B_w} \right). \tag{13}$$

For gas phase,

$$\nabla \cdot \left[\frac{K(p) K_{\mathrm{rg}}}{B_g \mu_g} \left(\nabla p_g - \lambda_g \right) \right] + \frac{q_g}{\rho_{\mathrm{gsc}}} = \frac{\partial}{\partial t} \left(\frac{\phi S_g}{B_g} \right). \tag{14}$$

Multiply the right term of (13) and (14), $(\partial/\partial t)(\phi S_w/B_w)$ and $(\partial/\partial t)(\phi S_g/B_g)$, with B_w and B_g, respectively, and then combine them together as follows:

$$\begin{aligned} & B_g \frac{\partial}{\partial t} \left(\frac{\phi S_g}{B_g} \right) + B_w \frac{\partial}{\partial t} \left(\frac{\phi S_w}{B_w} \right) \\ &= \phi \frac{\partial S_g}{\partial t} + S_g \frac{\partial \phi}{\partial p_g} \frac{\partial p_g}{\partial t} - \frac{\phi S_g}{B_g} \frac{\partial B_g}{\partial p_g} \frac{\partial p_g}{\partial t} - \phi \frac{\partial S_g}{\partial t} \\ &\quad + S_w \frac{\partial \phi}{\partial p_g} \frac{\partial p_g}{\partial t} - \frac{\phi S_w}{B_w} \frac{\partial B_w}{\partial p_g} \frac{\partial p_g}{\partial t} \\ &= \left(S_w + S_g \right) \frac{\partial \phi}{\partial p_g} \frac{\partial p_g}{\partial t} - \phi S_w \frac{1}{B_w} \frac{\partial B_w}{\partial p_g} \frac{\partial p_g}{\partial t} \\ &\quad - \phi S_g \frac{1}{B_g} \frac{\partial B_g}{\partial p_g} \frac{\partial p_g}{\partial t} \\ &= \frac{\partial \phi}{\partial p_g} \frac{\partial p_g}{\partial t} + \phi S_w \left(-\frac{1}{B_w} \frac{\partial B_w}{\partial p_g} \frac{\partial p_g}{\partial t} \right) \\ &\quad - \phi S_g \frac{1}{B_g} \frac{\partial B_g}{\partial p_g} \frac{\partial p_g}{\partial t}. \end{aligned} \tag{15}$$

According to the definition of compressibility, the compressibility of water, gas, and rock can be written as follows:

$$\begin{aligned} C_w &= -\frac{1}{B_w} \frac{\partial B_w}{\partial p_g} \\ C_g &= -\frac{1}{B_g} \frac{\partial B_w}{\partial p_g} \\ C_r &= \frac{1}{\phi} \frac{\partial \phi}{\partial \overline{p}} = \frac{1}{\phi} \frac{\partial \phi}{\partial p_g} \\ C_t &= C_r + C_g S_g + C_w S_w \\ \frac{\partial \phi}{\partial p_g} \frac{\partial p_g}{\partial t} &= \frac{\partial \phi}{\partial \overline{p}} \frac{\partial \overline{p}}{\partial t}. \end{aligned} \tag{16}$$

Therefore, (15) can be rewritten as

$$\begin{aligned} & \frac{\partial \phi}{\partial p_g} \frac{\partial p_g}{\partial t} + \phi S_w \left(-\frac{1}{B_w} \frac{\partial B_w}{\partial p_g} \frac{\partial p_g}{\partial t} \right) - \phi S_g \frac{1}{B_g} \frac{\partial B_g}{\partial p_g} \frac{\partial p_g}{\partial t} \\ &= \phi \left[\frac{1}{\phi} \frac{\partial \phi}{\partial p_g} \frac{\partial p_g}{\partial t} + S_w \left(-\frac{1}{B_w} \frac{\partial B_w}{\partial p_g} \frac{\partial p_g}{\partial t} \right) \right. \\ &\quad \left. - \frac{S_g}{B_g} \frac{\partial B_g}{\partial p_g} \frac{\partial p_g}{\partial t} \right] = \phi \left[\frac{1}{\phi} \frac{\partial \phi}{\partial p_g} + S_w \left(-\frac{1}{B_w} \frac{\partial B_w}{\partial p_g} \right) \right. \end{aligned}$$

$$+ S_g\left(-\frac{1}{B_g}\frac{\partial B_g}{\partial p_g}\right)\Bigg]\frac{\partial p_g}{\partial t} = \phi\left(C_r + C_w S_w + C_g S_g\right)\frac{\partial p_g}{\partial t} = \phi C_t \frac{\partial p_g}{\partial t}. \tag{17}$$

By combining the above equations, it yields the basic differential equation in the following form:

$$\begin{aligned} &B_g\nabla\cdot\left(\frac{K(p)K_{\mathrm{rg}}}{B_g\mu_g}\nabla p_g\right) - B_g\nabla\cdot\left(\frac{K(p)K_{\mathrm{rg}}}{B_g\mu_g}\lambda_g\right) \\ &+ B_g\frac{q_g}{\rho_{\mathrm{gsc}}} + B_w\nabla\cdot\left(\frac{K(p)K_{\mathrm{rw}}}{B_w\mu_w}\nabla p_g\right) - B_w\nabla \\ &\cdot\left(\frac{K(p)K_{\mathrm{rw}}}{B_w\mu_w}\nabla p_{\mathrm{cgw}}\right) - B_w\nabla\cdot\left(\frac{K(p)K_{\mathrm{rw}}}{B_w\mu_w}\lambda_w\right) \\ &+ B_w\frac{q_w}{\rho_{\mathrm{wsc}}} = \phi C_t\frac{\partial p_g}{\partial t}. \end{aligned} \tag{18}$$

4. Model Discretization and Solution

For the simplicity of model solution, pressure, p, is used to substitute the gas phase pressure p_g and M_i is introduced into the calculation:

$$M_i = \frac{K_{\mathrm{rl}}}{\mu_l B_l}, \quad \text{where } i = g, w. \tag{19}$$

4.1. Pressure Term

$$\begin{aligned} V_{i,j,k}\nabla\cdot\left(K(p)M_g\nabla p\right) &= \frac{\partial}{\partial x}\left[K(p)M_g\frac{\partial p}{\partial x}\right] + \frac{\partial}{\partial y}\left[K(p)M_g\frac{\partial p}{\partial y}\right] + \frac{\partial}{\partial z}\left[K(p)M_g\frac{\partial p}{\partial z}\right] \\ &= \Delta y_j\Delta z_k\left\{\left[K(p)M_g\right]_{i+1/2}\frac{p_{i+1}^{n+1}-p_i^{n+1}}{\Delta x_{i+1/2}} - \left[K(p)M_g\right]_{i-1/2}\frac{p_i^{n+1}-p_{i-1}^{n+1}}{\Delta x_{i-1/2}}\right\} \\ &+ \Delta x_i\Delta z_k\left\{\left[K(p)M_g\right]_{j+1/2}\frac{p_{j+1}^{n+1}-p_j^{n+1}}{\Delta y_{j+1/2}} - \left[K(p)M_g\right]_{j-1/2}\frac{p_j^{n+1}-p_{j-1}^{n+1}}{\Delta y_{j-1/2}}\right\} \\ &+ \Delta x_i\Delta y_j\left\{\left[K(p)M_g\right]_{k+1/2}\frac{p_{k+1}^{n+1}-p_k^{n+1}}{\Delta z_{k+1/2}} - \left[K(p)M_g\right]_{k-1/2}\frac{p_k^{n+1}-p_{k-1}^{n+1}}{\Delta z_{k-1/2}}\right\}. \end{aligned} \tag{20}$$

The complete subscript of (20) is expressed as follows:

$$\begin{aligned} \Delta x_i &= \Delta x_{i,j,k} \\ \left[K(p)M_g\right]_{i+1/2} &= \left[K(p)M_g\right]_{i+1/2,j,k} \\ \frac{p_{i+1}^{n+1}-p_i^{n+1}}{\Delta x_{i+1/2}} &= \frac{p_{i+1,j,k}^{n+1}-p_{i,j,k}^{n+1}}{\Delta x_{i+1/2,j,k}} \\ V_{i,j,k} &= \Delta x_i\Delta y_j\Delta z_k. \end{aligned} \tag{21}$$

The pressure term for water phase can also be discretized likewise.

$$\begin{aligned} V_{i,j,k}\nabla\cdot\left(K(p)M_w\nabla p\right) &= \Delta y_j\Delta z_k\left\{\left[K(p)M_w\right]_{i+1/2}\frac{p_{i+1}^{n+1}-p_i^{n+1}}{\Delta x_{i+1/2}} - \left[K(p)M_w\right]_{i-1/2}\frac{p_i^{n+1}-p_{i-1}^{n+1}}{\Delta x_{i-1/2}}\right\} \\ &+ \Delta x_i\Delta z_k\left\{\left[K(p)M_w\right]_{j+1/2}\frac{p_{j+1}^{n+1}-p_j^{n+1}}{\Delta y_{j+1/2}} - \left[K(p)M_w\right]_{j-1/2}\frac{p_j^{n+1}-p_{j-1}^{n+1}}{\Delta y_{j-1/2}}\right\} \\ &+ \Delta x_i\Delta y_j\left\{\left[K(p)M_w\right]_{k+1/2}\frac{p_{k+1}^{n+1}-p_k^{n+1}}{\Delta z_{k+1/2}} - \left[K(p)M_w\right]_{k-1/2}\frac{p_k^{n+1}-p_{k-1}^{n+1}}{\Delta z_{k-1/2}}\right\}. \end{aligned} \tag{22}$$

The pressure term in percolation formulation can be written as

$$\begin{aligned} &h_{i,j,k}p_{i,j,k-1}^{n+1} + a_{i,j,k}p_{i,j-1,k}^{n+1} + b_{i,j,k}p_{i-1,j,k}^{n+1} + c_{i,j,k}p_{i,j,k}^{n+1} \\ &\quad + f_{i,j,k}p_{i+1,j,k}^{n+1} + e_{i,j,k}p_{i,j+1,k}^{n+1} + l_{i,j,k}p_{i,j,k+1}^{n+1}, \end{aligned} \tag{23}$$

where

$$\begin{aligned} h_{i,j,k} &= \frac{\Delta x_i\Delta y_j}{\Delta z_{k-1/2}}\left\{B_g\left[K(p)M_g\right]_{k-1/2} + B_w\left[K(p)M_w\right]_{k-1/2}\right\} \\ a_{i,j,k} &= \frac{\Delta x_i\Delta z_k}{\Delta y_{j-1/2}}\left\{B_g\left[K(p)M_g\right]_{j-1/2} + B_w\left[K(p)M_w\right]_{j-1/2}\right\} \\ b_{i,j,k} &= \frac{\Delta y_j\Delta z_k}{\Delta x_{i-1/2}}\left\{B_g\left[K(p)M_g\right]_{i-1/2} + B_w\left[K(p)M_w\right]_{i-1/2}\right\} \end{aligned}$$

$$
\begin{aligned}
f_{i,j,k} &= \frac{\Delta y_j \Delta z_k}{\Delta x_{i+1/2}} \left\{ B_g \left[K(p) M_g \right]_{i+1/2} \right. \\
&\quad \left. + B_w \left[K(p) M_w \right]_{i+1/2} \right\} \\
e_{i,j,k} &= \frac{\Delta x_i \Delta z_k}{\Delta y_{j+1/2}} \left\{ B_g \left[K(p) M_g \right]_{j+1/2} \right. \\
&\quad \left. + B_w \left[K(p) M_w \right]_{j+1/2} \right\} \\
l_{i,j,k} &= \frac{\Delta x_i \Delta y_j}{\Delta z_{k+1/2}} \left\{ B_g \left[K(p) M_g \right]_{k+1/2} \right. \\
&\quad \left. + B_w \left[K(p) M_w \right]_{k+1/2} \right\} \\
c_{i,j,k} &= -\left(b_{i,j,k} + f_{i,j,k} + a_{i,j,k} + e_{i,j,k} + h_{i,j,k} + l_{i,j,k} \right).
\end{aligned} \tag{24}
$$

4.2. TPG Term. The TPG term for gas phase can be written as

$$
\begin{aligned}
&- B_g \nabla \cdot \left(\frac{K(p) K_{\mathrm{rg}}}{B_g \mu_g} \lambda_g \right) \cdot V_{i,j,k} \\
&\quad = \overline{H}_{i,j,k} \frac{1}{2} \left(\lambda_{gzk-1} \Delta z_{k-1} + \lambda_{gzk} \Delta z_k \right) \\
&\qquad + \overline{A}_{i,j,k} \frac{1}{2} \left(\lambda_{gyj-1} \Delta z_{j-1} + \lambda_{gyj} \Delta z_j \right) \\
&\qquad + \overline{B}_{i,j,k} \frac{1}{2} \left(\lambda_{gxi-1} \Delta z_{i-1} + \lambda_{gxi} \Delta z_i \right) \\
&\qquad + \overline{F}_{i,j,k} \frac{1}{2} \left(\lambda_{gxi+1} \Delta z_{i+1} + \lambda_{gxi} \Delta z_i \right) \\
&\qquad + \overline{E}_{i,j,k} \frac{1}{2} \left(\lambda_{gyj+1} \Delta z_{j+1} + \lambda_{gyj} \Delta z_j \right) \\
&\qquad + \overline{L}_{i,j,k} \frac{1}{2} \left(\lambda_{gzk+1} \Delta z_{k+1} + \lambda_{gzk} \Delta z_k \right),
\end{aligned} \tag{25}
$$

where

$$
\begin{aligned}
\overline{H}_{i,j,k} &= \frac{\Delta x_i \Delta y_j}{\Delta z_{k-1/2}} \left\{ B_g \left[K(p) M_g \right]_{k-1/2} \right\} \\
\overline{A}_{i,j,k} &= \frac{\Delta x_i \Delta z_k}{\Delta y_{j-1/2}} \left\{ B_g \left[K(p) M_g \right]_{j-1/2} \right\} \\
\overline{B}_{i,j,k} &= \frac{\Delta y_j \Delta z_k}{\Delta x_{i-1/2}} \left\{ B_g \left[K(p) M_g \right]_{i-1/2} \right\} \\
\overline{F}_{i,j,k} &= -\frac{\Delta y_j \Delta z_k}{\Delta x_{i+1/2}} \left\{ B_g \left[K(p) M_g \right]_{i+1/2} \right\} \\
\overline{E}_{i,j,k} &= -\frac{\Delta x_i \Delta z_k}{\Delta y_{j+1/2}} \left\{ B_g \left[K(p) M_g \right]_{j+1/2} \right\} \\
\overline{L}_{i,j,k} &= -\frac{\Delta x_i \Delta y_j}{\Delta z_{k+1/2}} \left\{ B_g \left[K(p) M_g \right]_{k+1/2} \right\}.
\end{aligned} \tag{26}
$$

The TPG term for water phase can be discretized likewise.

4.3. Capillary Pressure Term. The capillary pressure term could be written as

$$
\begin{aligned}
&- B_w \nabla \cdot \left(\frac{K(p) K_{\mathrm{rw}}}{B_w \mu_w} \nabla p_{\mathrm{cgw}} \right) \cdot V_{i,j,k} \\
&\quad = \overline{h}_{i,j,k} p^{n+1}_{\mathrm{cgwi},j,k-1} + \overline{a}_{i,j,k} p^{n+1}_{\mathrm{cgwi},j-1,k} + \overline{b}_{i,j,k} p^{n+1}_{\mathrm{cgwi}-1,j,k} \\
&\qquad + \overline{c}_{i,j,k} p^{n+1}_{\mathrm{cgwi},j,k} + \overline{f}_{i,j,k} p^{n+1}_{\mathrm{cgwi}+1,j,k} + \overline{e}_{i,j,k} p^{n+1}_{\mathrm{cgwi},j+1,k} \\
&\qquad + \overline{l}_{i,j,k} p^{n+1}_{\mathrm{cgwi},j,k+1},
\end{aligned} \tag{27}
$$

where

$$
\begin{aligned}
\overline{h}_{i,j,k} &= -\frac{\Delta x_i \Delta y_j}{\Delta z_{k-1/2}} \left\{ B_w \left[K(p) M_w \right]_{k-1/2} \right\} \\
\overline{a}_{i,j,k} &= -\frac{\Delta x_i \Delta z_k}{\Delta y_{j-1/2}} \left\{ B_w \left[K(p) M_w \right]_{j-1/2} \right\} \\
\overline{b}_{i,j,k} &= -\frac{\Delta y_j \Delta z_k}{\Delta x_{i-1/2}} \left\{ B_w \left[K(p) M_w \right]_{i-1/2} \right\} \\
\overline{f}_{i,j,k} &= -\frac{\Delta y_j \Delta z_k}{\Delta x_{i+1/2}} \left\{ B_w \left[K(p) M_w \right]_{i+1/2} \right\} \\
\overline{e}_{i,j,k} &= -\frac{\Delta x_i \Delta z_k}{\Delta y_{j+1/2}} \left\{ B_w \left[K(p) M_w \right]_{j+1/2} \right\} \\
\overline{l}_{i,j,k} &= -\frac{\Delta x_i \Delta y_j}{\Delta z_{k+1/2}} \left\{ B_w \left[K(p) M_w \right]_{k+1/2} \right\} \\
\overline{c}_{i,j,k} &= -\left(\overline{b}_{i,j,k} + \overline{f}_{i,j,k} + \overline{a}_{i,j,k} + \overline{e}_{i,j,k} + \overline{h}_{i,j,k} + \overline{l}_{i,j,k} \right).
\end{aligned} \tag{28}
$$

4.4. Cumulative Term. The forward-differentiation method is used to deal with the cumulative term.

$$
\phi C_t \frac{\partial p}{\partial t} = \phi C_t \frac{p^{n+1}_{i,j,k} - p^n_{i,j,k}}{\Delta t}. \tag{29}
$$

4.5. Differential Equation

$$
\begin{aligned}
&h_{i,j,k} p^{n+1}_{i,j,k-1} + a_{i,j,k} p^{n+1}_{i,j-1,k} + b_{i,j,k} p^{n+1}_{i-1,j,k} \\
&\qquad + \left(c_{i,j,k} - V_{i,j,k} \frac{\phi C_t}{\Delta t} \right) p^{n+1}_{i,j,k} + f_{i,j,k} p^{n+1}_{i+1,j,k} \\
&\qquad + e_{i,j,k} p^{n+1}_{i,j+1,k} + l_{i,j,k} p^{n+1}_{i,j,k+1} \\
&\quad = -\overline{h}_{i,j,k} p^{n+1}_{\mathrm{cgwi},j,k-1} - \overline{a}_{i,j,k} p^{n+1}_{\mathrm{cgwi},j-1,k} \\
&\qquad - \overline{b}_{i,j,k} p^{n+1}_{\mathrm{cgwi}-1,j,k} - \overline{c}_{i,j,k} p^{n+1}_{\mathrm{cgwi},j,k} - \overline{f}_{i,j,k} p^{n+1}_{\mathrm{cgwi}+1,j,k} \\
&\qquad - \overline{e}_{i,j,k} p^{n+1}_{\mathrm{cgwi},j+1,k} - \overline{l}_{i,j,k} p^{n+1}_{\mathrm{cgwi},j,k+1} \\
&\qquad - \overline{H}_{i,j,k} \frac{1}{2} \left(\lambda_{gzk-1} \Delta z_{k-1} + \lambda_{gzk} \Delta z_k \right) \\
&\qquad - \overline{A}_{i,j,k} \frac{1}{2} \left(\lambda_{gyj-1} \Delta z_{j-1} + \lambda_{gyj} \Delta z_j \right)
\end{aligned}
$$

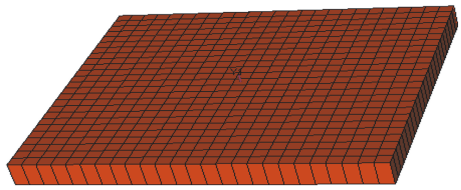

Figure 5: The schematic for the simulation model.

$$
\begin{aligned}
&- \overline{B}_{i,j,k} \frac{1}{2} \left(\lambda_{gxi-1} \Delta z_{i-1} + \lambda_{gxi} \Delta z_i \right) \\
&- \overline{F}_{i,j,k} \frac{1}{2} \left(\lambda_{gxi+1} \Delta z_{i+1} + \lambda_{gxi} \Delta z_i \right) \\
&- \overline{E}_{i,j,k} \frac{1}{2} \left(\lambda_{gyj+1} \Delta z_{j+1} + \lambda_{gyj} \Delta z_j \right) \\
&- \overline{L}_{i,j,k} \frac{1}{2} \left(\lambda_{gzk+1} \Delta z_{k+1} + \lambda_{gzk} \Delta z_k \right) \\
&- \overline{H}'_{i,j,k} \frac{1}{2} \left(\lambda_{wzk-1} \Delta z_{k-1} + \lambda_{wzk} \Delta z_k \right) \\
&- \overline{A}'_{i,j,k} \frac{1}{2} \left(\lambda_{wyj-1} \Delta z_{j-1} + \lambda_{wyj} \Delta z_j \right) \\
&- \overline{B}'_{i,j,k} \frac{1}{2} \left(\lambda_{wxi-1} \Delta z_{i-1} + \lambda_{wxi} \Delta z_i \right) \\
&- \overline{F}'_{i,j,k} \frac{1}{2} \left(\lambda_{wxi+1} \Delta z_{i+1} + \lambda_{wxi} \Delta z_i \right) \\
&- \overline{E}'_{i,j,k} \frac{1}{2} \left(\lambda_{wyj+1} \Delta z_{j+1} + \lambda_{wyj} \Delta z_j \right) \\
&- \overline{L}'_{i,j,k} \frac{1}{2} \left(\lambda_{wzk+1} \Delta z_{k+1} + \lambda_{wzk} \Delta z_k \right) - V_{i,j,k} \\
&\cdot \left(B_g \frac{q_g}{\rho_{\mathrm{gsc}}} + B_w \frac{q_w}{\rho_{\mathrm{wsc}}} \right) - V_{i,j,k} \phi C_t \frac{p^n_{i,j,k}}{\Delta t}.
\end{aligned}
\tag{30}
$$

Equation (30) is the basic differential equation after discretization. The coefficient matrix of (30) is a seven-diagonal matrix with diagonal dominance. After the pressure of the gas phase is obtained through an implicit method, the pressure of the water phase can be obtained through capillary pressure explicitly. The relative permeability, threshold pressure gradient, and permeability under stress could be obtained through an explicit method.

5. Results and Discussion

5.1. Model Validation. A numerical model was built to simulate a homogeneous water-bearing tight gas reservoir of the Ordos Basin, located in Northwest China. The simulated vertical well is located at the center of the model, as shown in Figure 5. At the start of the simulation, we let the gas well produce at constant rate; when the bottom-hole pressure reaches a certain value, the production regime switches to constant bottom-hole pressure. Basic parameters for the model calculation are listed in Table 1. The nonlinear percolation parameters in the Appendix are chosen according to the experiment results in Section 1.

Table 1: Basic model parameters.

Reservoir area, m^2	202500
Reservoir depth, m	3300
Initial formation pressure, MPa	30.5
Porosity, %	8.5
Permeability, mD	0.1
Initial water saturation	0.40
Number of grid blocks	$15 \times 15 \times 1$
Step size of a block (DX, DY, DZ), m	30, 30, 10
Half-length of hydraulic fracture, m	100
Permeability of the hydraulic fracture, mD	50
Bottom hole pressure, MPa	5

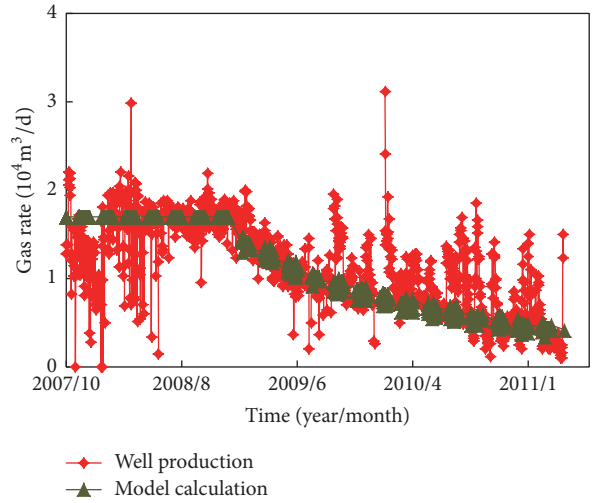

Figure 6: The comparison between well production and results of model calculation.

The new numerical model is validated by comparing with the actual well performance. The results of comparison are shown in Figure 6. We can see from Figure 6 that the numerical model runs according to the setting regimes strictly. The model has a high accuracy at the period of constant bottom-hole pressure, although the initial production presents discrepancy with the actual gas rate, which can be explained by the actual varied production regimes. In general, there is a relatively high accuracy for the new numerical model.

5.2. The Effect of TPG. In order to analyze the influence of TPG to well productivity, the daily production rate and cumulative gas production are separately compared for the cases with and without considering TPG. The results of the simulation are shown in Figures 7 and 8. When neglecting the TPG, the gas production plateau can last 1201 days and the gas recovery during this stage is 54.39%. The ultimate gas recovery without TPG reaches 81.85%. While the TPG is taken into account, the period of stable production reduces to

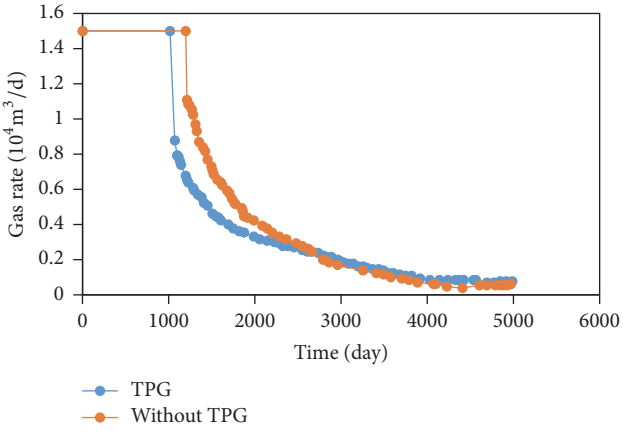

Figure 7: Effect of TPG on gas production.

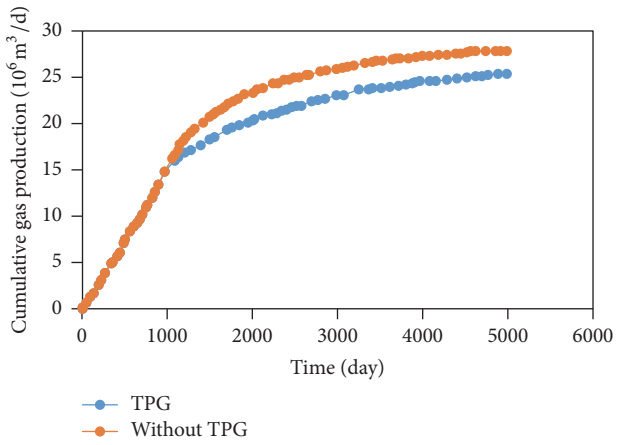

Figure 8: Effect of TPG on cumulative gas production.

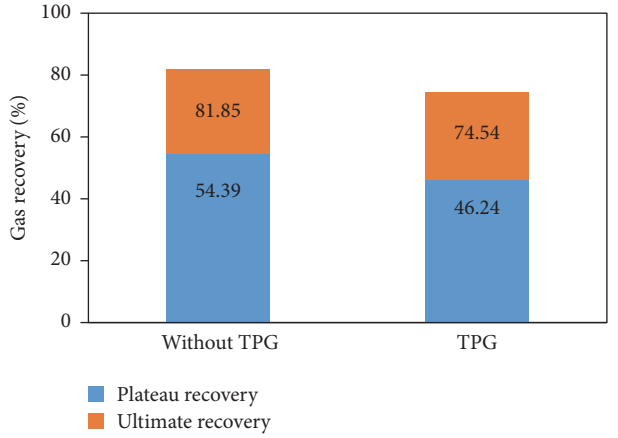

Figure 9: Gas recovery of different periods with or without TPG.

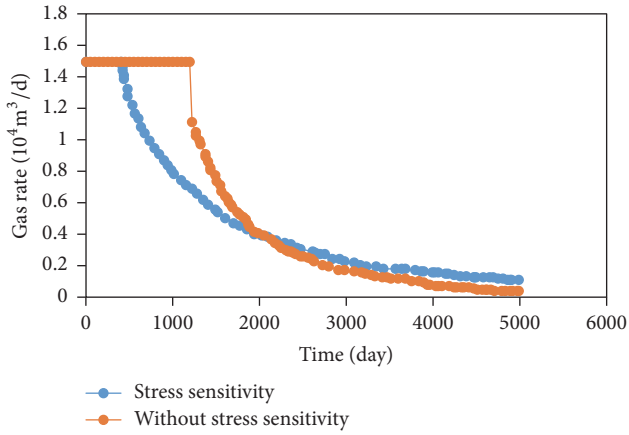

Figure 10: Effect of stress sensitivity on gas production.

1021 days and the gas recovery during this period decreases to 46.24%. The ultimate recovery with TPG is 74.54%, as shown in Figure 9. To sum up, when the TPG is included in the model, the production plateau will shrink and the gas recovery for both the stabilized production stage and the final recovery will decrease.

5.3. The Effect of Stress Sensitivity. The impact of stress sensitivity on gas productivity is simulated and the results are shown in Figures 10 and 11. When the stress sensitivity is considered, the production plateau reduces to 421 days and the gas recovery during this period is just 19.06%. The ultimate gas recovery of the simulation is 73.58%, as shown in Figure 12. Overall, the stabilized production stage reduces and the gas recovery decreases when the stress effect is considered.

5.4. The Joint Effect of TPG and Stress Sensitivity. When a gas well is put into production, both the TPG and stress sensitivity will have an effect on the gas productivity. The influence of the two factors to gas production is simulated and results are shown in Figures 13 and 14. It is seen that the production plateau reduces sharply from 1201 days to 61 days and the gas recovery during this period shrinks to 2.76%. The ultimate gas recovery is also severely affected and decreases to 55.49%, as shown in Figure 15. However, compared with gas recovery of the stabilized stage, the gas recovery of declining period is influenced by TPG and stress sensitivity relatively moderately. Therefore, TPG and stress sensitivity mainly infringe the duration and gas recovery of the stabilized period.

5.5. The Effect of Primary Water Saturation. Well performance under different primary water saturations varies tremendously. We analyze the impact of water presence to gas well by setting the water saturation from 40% to 55%. The initial daily gas rate is set to be 1.5×10^4 m^3/d. The results are shown in Figures 16, 17, 18, and 19. It can be seen that, with the increase of the primary water saturation, the stabilized production period will be shorten, gas decline rate will slow down, and the gas recovery will decrease. In addition, the water rate will increase with the water saturation. In the case of the highest water saturation, the water rate accelerates fastest and reaches peak earliest. As for the gas-water ratio, when the water saturation is larger than 50%, the ratio will

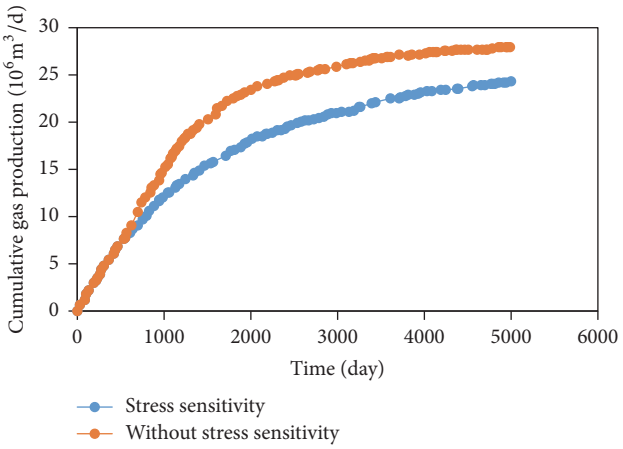

Figure 11: Effect of stress sensitivity on cumulative gas production.

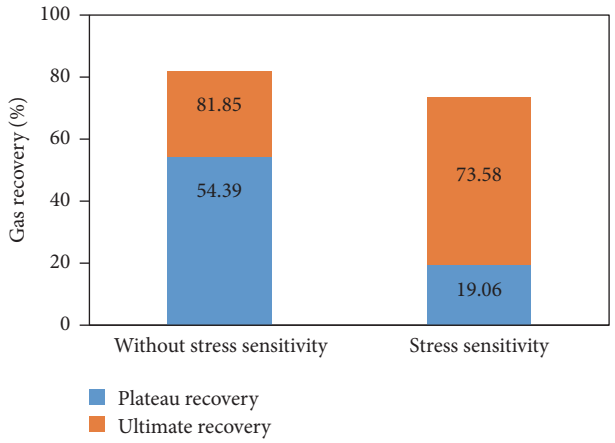

Figure 12: Gas recovery of different periods with or without stress sensitivity.

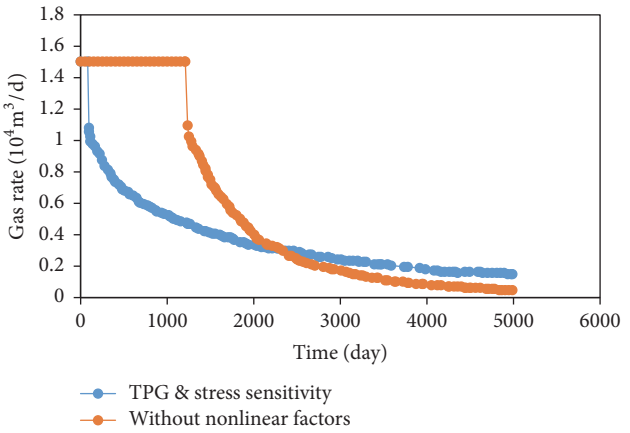

Figure 13: Effect of nonlinear factors on gas production.

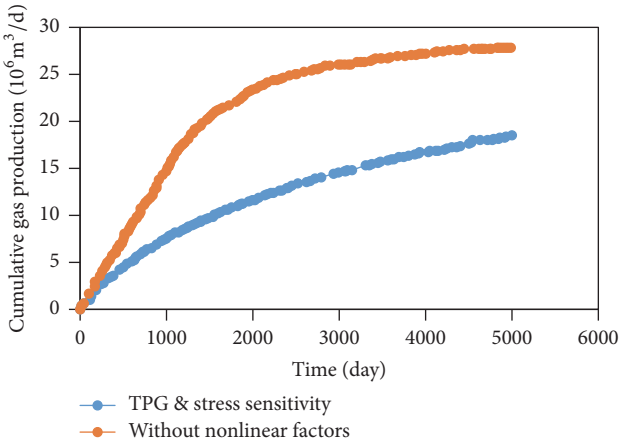

Figure 14: Effect of nonlinear factors on cumulative gas production.

increase sharply as the production continues. Therefore, during the production process, reasonable drawdown pressure should be set to control the water transportation within formation so that the water accumulation could be avoided.

5.6. The Effect of Displacement Pressure Gradient. According to the pervious experiments, the pressure gradient will affect gas-water relative permeability. The pressure distribution of different production regimes has been simulated, as shown in Figure 20. As seen, the pressure gradient needed for gas flow is small and most of the simulated region contains pressure gradient less than 10.2 MPa/m. Only when the pressure gradient is greater than 10.2 MPa/m, the gas-water permeability will change. Therefore, the pressure gradient will have little effect on gas recovery through its influence on gas-water relative permeability.

6. Measurements for Enhanced Gas Recovery

From the above influential factor analysis, the gas productivity and recovery are greatly impacted by water saturation, TPG, and stress sensitivity. In order to obtain the optimal gas productivity, the development of water-bearing tight gas reservoirs should be optimized in several fronts, such as the well pattern, well location, and production regimes.

(1) Water should be avoided during the production process. Recognition of water saturation distribution is essential so that the high water saturation region should be detected and kept away.

(2) Due to the high stress sensitivity of tight gas reservoirs, the pressure drawdown near wellbore should be kept reasonable. In comparison with vertical wells, a fractured horizontal well could decrease the pressure drawdown efficiently and reduce the formation damage from stress.

(3) If the bottom-hole pressure is too low, the stress sensitivity near wellbore will be severe and the formation will be damaged. If the bottom-hole pressure is too high, the gas rate will be too small though the damage of stress could be prevented. Therefore, the drawdown pressure and gas rate need to be optimized so that the damage of stress could be minimized and gas recovery could be maximized.

Based on the parameters in Table 1, several cases with various gas rates have been simulated, and the results are shown in Table 2 and Figures 21–25. By increasing the gas rate,

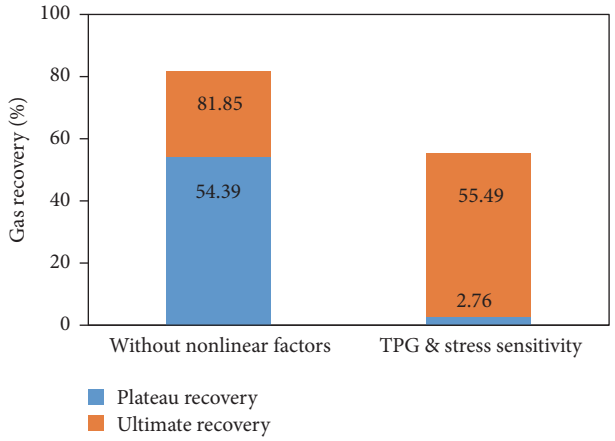

Figure 15: Gas recovery of different periods with or without TPG and stress sensitivity.

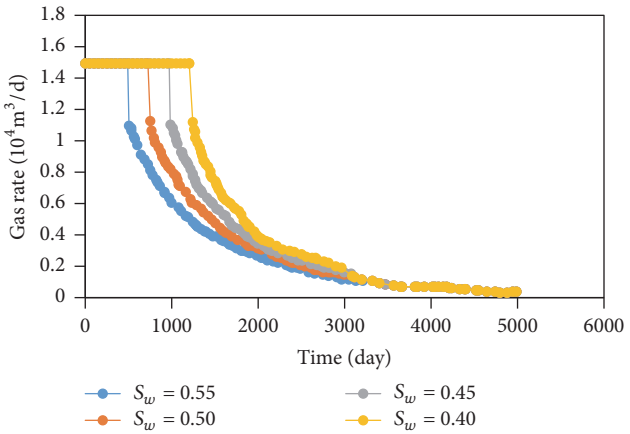

Figure 16: Effect of water saturation on gas production.

Table 2: Stabilized production period and gas recovery under different gas rates.

Gas rate (10^4 m^3/d)	Stabilized production period (year)	Cumulative gas production (10^6 m^3)	Ultimate gas recovery (%)
1	5.7	27.18	82.06
1.5	3.3	27.11	81.85
2	2.2	27.06	81.71
3	1.2	26.95	81.37
4	0.7	26.55	80.15

the production plateau will be shortened sharply and the gas recovery will decrease as a result. If a stabilized production period of 2 or 3 years is aimed, the gas rate should be no more than 2×10^4 m^3/d.

When the bottom-hole pressure reaches the initial critical value, the gas rate will decline quickly as shown in Figure 22. When the gas rate is 1.0×10^4 m^3/d, though a relatively longer plateau and higher gas recovery could be obtained, the cumulative production stays lower during most of the simulation process. When the gas rate is larger than 2×10^4 m^3/d, the increase of cumulative gas recovery is limited (Figure 23).

From Figures 26 and 27, when gas rate increases, the water rate increases greatly and the time of peak water rate

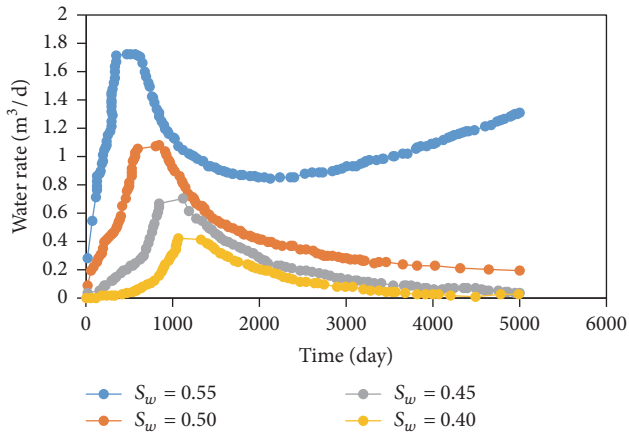

Figure 17: Effect of water saturation on water production.

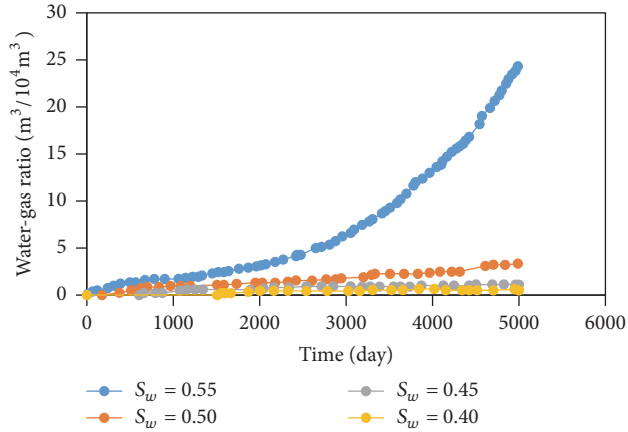

Figure 18: Effect of water saturation on gas-water ratio.

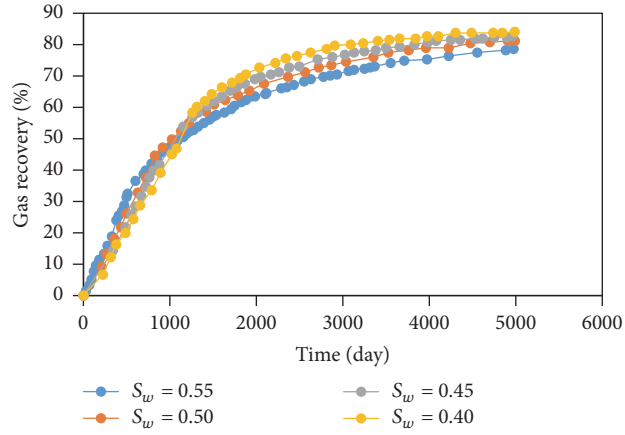

Figure 19: Effect of water saturation on gas recovery.

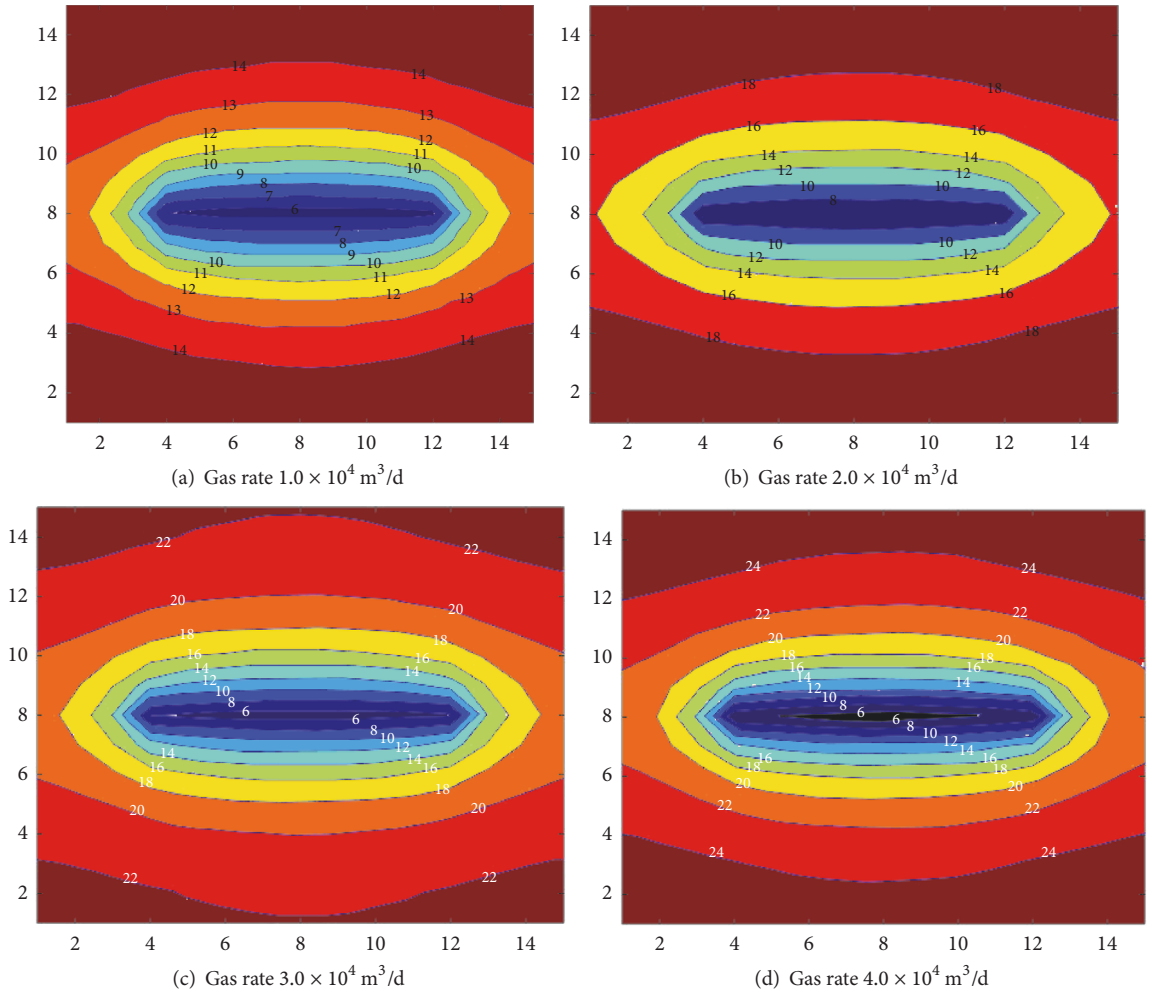

(a) Gas rate 1.0×10^4 m^3/d (b) Gas rate 2.0×10^4 m^3/d

(c) Gas rate 3.0×10^4 m^3/d (d) Gas rate 4.0×10^4 m^3/d

FIGURE 20: The pressure distribution after stabilized production stage under different gas rates.

is advanced; in addition, the trend of gas-water ratio will rise sharply and the value of gas-water ratio will increase.

7. Conclusions

A gas-water two-phase flow model is proposed, and it is applicable to tight gas reservoirs based on the percolation characteristics of tight gas reservoirs and with consideration of the effect of nonlinear factors on gas well production. When considering threshold pressure and media deformation, the duration of the plateau production period and gas recovery decreases. Notice also that the media deformation has a more significant effect on well production than the threshold pressure. In summary, the following points are drawn from this study.

(1) Water is basically immobile when the primary water saturation is small. The plateau reduces with the increase of drawdown pressure. The productivity of gas well decreases sharply when the bottom-hole pressure reaches the initial critical pressure and the gas well produces at constant pressure.

(2) Presence of water changes the gas percolation. When there is high water saturation within the formation and gas-water two-phase flow takes place, gas-water ratio increases with the drawdown pressure. Therefore, reasonable drawdown pressure should be set in a gas reservoir with high water saturation.

(3) When the stress sensitivity and TPG are considered, the plateau will be shortened and gas recovery during the period will decrease. In comparison with TPG, stress sensitivity has a larger effect on gas productivity.

(4) Pressure gradient has an effect on gas-water permeability. However, for a gas reservoir, if the drawdown pressure gradient is limited, the effect of gas-water permeability on gas productivity could be negligible (or small).

(5) Water should be prevented and reasonable drawdown pressure should be kept as possible during the gas production in order to optimize gas recovery.

Appendix

Simulation Parameters

TPG and permeability have a power relationship:

$$\lambda = aK^{b(1-S_w)}e^{S_w}, \tag{A.1}$$

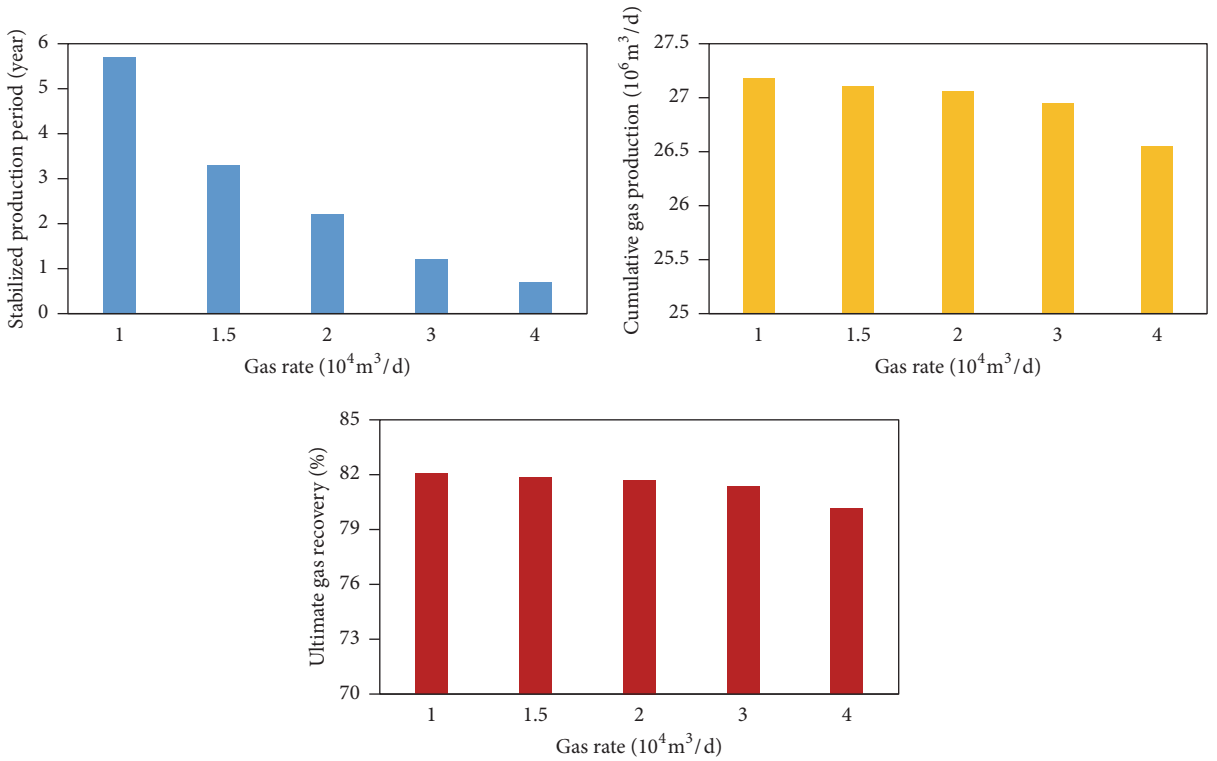

FIGURE 21: The stabilized production period, cumulative gas production, and gas recovery under different gas rates.

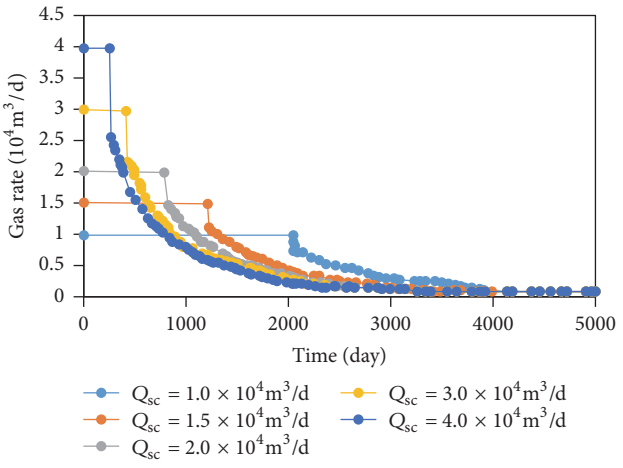

FIGURE 22: Gas rate under different initial gas rates.

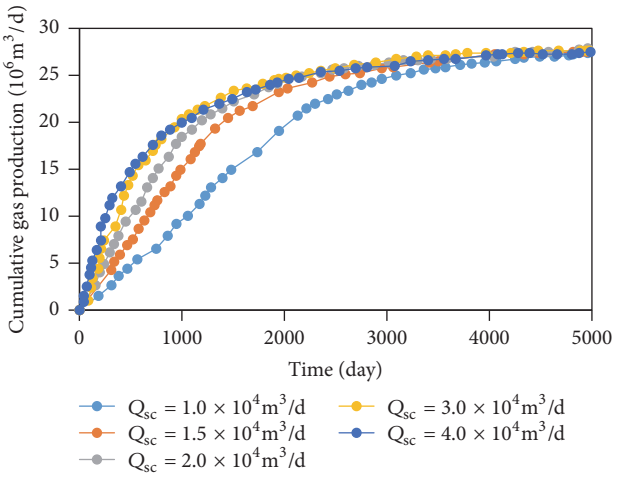

FIGURE 23: Cumulative gas production under different initial gas rates.

where a and S_w also have a power relation:

$$a = 2 \times 10^{-9} \times e^{(28.268 \cdot S_w)}. \tag{A.2}$$

And b and S_w have a linear relation:

$$b = 3.576 \cdot S_w + 3.2692. \tag{A.3}$$

Therefore, the relationship between permeability and water saturation is

$$\lambda_g = 2 \times 10^{-9} \times e^{(28.268 \cdot S_w)} K^{(3.576 \cdot S_w - 3.2692)}. \tag{A.4}$$

The stress sensitivity coefficient is

$$S_p = a e^{bS_w} = \frac{1}{2} c \left(K_i\right)^{-n} e^{(-31.96K_i + 4.12)S_w}, \tag{A.5}$$

where $c = 0.2373$, $n = 0.3015$.

The threshold pressure gradient is

$$\lambda_g = 2 \times 10^{-9} \times e^{(28.268 \cdot S_w)} K^{(3.576 \cdot S_w - 3.2692)}. \tag{A.6}$$

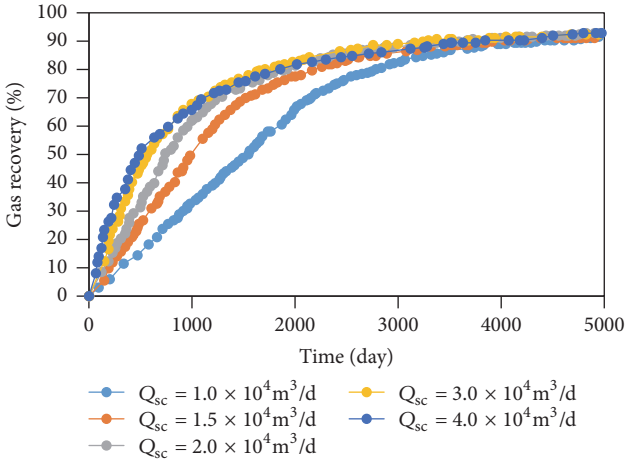

Figure 24: Gas recovery under different initial gas rates.

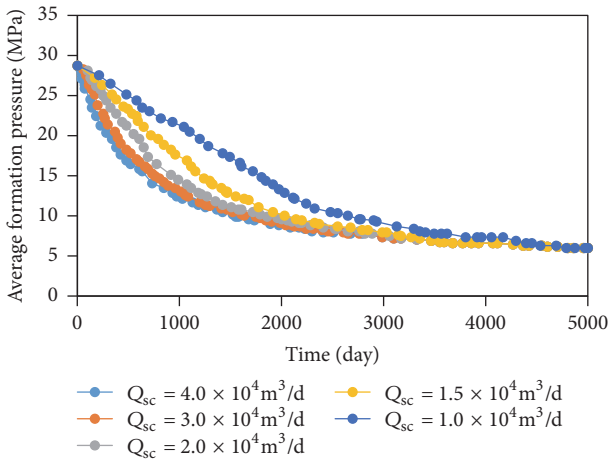

Figure 25: Average formation pressure under different initial gas rates.

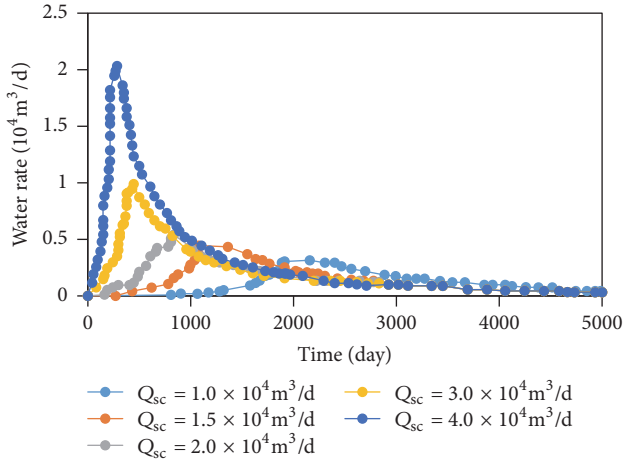

Figure 26: Water rate under different initial gas rates.

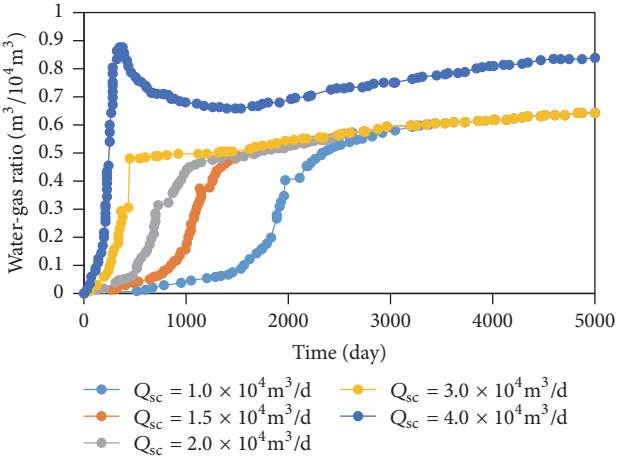

Figure 27: Gas-water ratio under different initial gas rates.

The relative permeability is

$$
\begin{aligned}
S_{wD} &= \frac{S_w - S_{wc}}{1 - S_{wc} - \left(1 - S_{gr}\right)} \\
K_{rw} &= 0.325 \times S_{wD}^{2.087} \\
K_{rg} &= 0.293 \times \left(1 - S_{wD}\right)^{1.072} \\
K_{rw} &= 0.55 \times S_{wD}^{1.442} \\
K_{rg} &= 0.385 \times \left(1 - S_{wD}\right)^{1.564}.
\end{aligned}
\tag{A.7}
$$

Nomenclature

Bg, Bw: Volume factor, decimal
$K(p)$: Absolute permeability of the reservoir, μm^2
K_{rj}: Relative permeability
p_j: Pressure, MPa
p_{cgw}: Gas-water capillary pressure, MPa
S_j: Saturation
S_{wc}: Initial water saturation
S_{gr}: Residual gas saturation
C_t: Total compressibility
t: Time, s
V_j, V_{js}: Underground volume and surface volume, cm^3
$\vec{v}_j$: Percolation velocity, cm/s
$p^n_{i+1/2}$: At the nth time step, the pressure of position $(i + 1/2, j, k)$.

Greek Symbols

φ: Porosity
μ_j: Viscosity, mPa·s
λ_j: Threshold pressure gradient
ρ_j: Fluid density, g/cm^3

ρ_{gsc}, ρ_{wsc}: Density of gas and water under standard surface conditions, g/cm^3.

Subscript

g: Gas phase
w: Water phase.

Conflicts of Interest

The authors declare that there are no conflicts of interest regarding the publication of this article.

Acknowledgments

The authors are grateful to financial support of National Natural Science Foundation of China (no. 51674273), National Basic Research Program of China ("973 Program") (no. 2015CB250900), and Science Foundation of China University of Petroleum, Beijing (no. 2462015YQ0206).

References

[1] L. K. Thomas, D. L. Katz, and M. R. Tek, "Threshold pressure phenomena in porous media," *Society of Petroleum Engineers Journal*, vol. 8, no. 2, pp. 174–184, 1968.

[2] F. Boukadi, A. Bemani, M. Rumhy, and M. Kalbani, "Threshold pressure as a measure of degree of rock wettability and diagenesis in consolidated Omani limestone cores," *Marine and Petroleum Geology*, vol. 15, no. 1, pp. 33–39, 1998.

[3] X. Wei, L. Qun, G. Shusheng, H. Zhiming, and X. Hui, "Pseudo threshold pressure gradient to flow for low permeability reservoirs," *Petroleum Exploration and Development*, vol. 36, no. 2, pp. 232–236, 2009.

[4] W. Liu, J. Yao, and Y. Wang, "Exact analytical solutions of moving boundary problems of one-dimensional flow in semi-infinite long porous media with threshold pressure gradient," *International Journal of Heat and Mass Transfer*, vol. 55, no. 21-22, pp. 6017–6022, 2012.

[5] J. Lu, "Pressure behavior of a hydraulic fractured well in tight gas formation with threshold pressure gradient," in *Proceedings of the SPE Middle East Unconventional Gas Conference and Exhibition*, Society of Petroleum Engineers, January 2012.

[6] F. Civan, "Modeling gas flow through hydraulically-fractured shale-gas reservoirs involving molecular-to-inertial transport regimes and threshold-pressure gradient," in *Proceedings of the SPE Annual Technical Conference and Exhibition*, Society of Petroleum Engineers, October 2013.

[7] S. Q. Li, L. S. Cheng, X. S. Li et al., "Nonlinear seepage flow of ultralow permeability reservoirs," *Petroleum Exploration and Development*, vol. 35, no. 5, pp. 606–612, 2008.

[8] B. Q. Zeng, L. S. Cheng, and C. L. Li, "Low velocity non-linear flow in ultra-low permeability reservoir," *Journal of Petroleum Science and Engineering*, vol. 80, no. 1, pp. 1–6, 2011.

[9] Q. J. Liu, B. H. Liu, X. B. Li et al., "The effect of water saturation on gas slip factor by pore scale network modeling," in *Proceedings of the SCA 2002 Symposium*, pp. 22–25, Monterey, Calif, USA, 2002.

[10] J. Ding, S. Yang, X. Nie, and Z. Wang, "Dynamic threshold pressure gradient in tight gas reservoir," *Journal of Natural Gas Science and Engineering*, vol. 20, pp. 155–160, 2014.

[11] I. Fatt and D. H. Davis, "Reduction in permeability with overburden pressure," *Journal of Petroleum Technology*, vol. 4, no. 12, p. 16, 1952.

[12] R. D. Thomas and D. C. Ward, "Effect of overburden pressure and water saturation on gas permeability of tight sandstone cores," *Journal of Petroleum Technology*, vol. 24, no. 2, pp. 120–124, 1972.

[13] J. Vairogs and V. W. Rhoades, "Pressure transient tests in formations having stress-sensitive permeability," *Journal of Petroleum Technology*, vol. 25, no. 8, pp. 965–970, 1973.

[14] N. H. Kilmer, N. R. Morrow, and J. K. Pitman, "Pressure sensitivity of low permeability sandstones," *Journal of Petroleum Science and Engineering*, vol. 1, no. 1, pp. 65–81, 1987.

[15] S. C. Jones, "Two-point determinations of permeability and PV vs. net confining stress," *SPE Formation Evaluation*, vol. 3, no. 1, pp. 235–241, 1988.

[16] Z. L. Yu, S. S. Gao, and J. P. Liu, "Stress sensitivity of tight reservoir and its influence on oilfield development," *Acta Petrolei Sinica*, vol. 28, no. 4, article 018, 2007.

[17] F. O. Jones and W. W. Owens, "A laboratory study of low-permeability gas sands," *Journal of Petroleum Technology*, vol. 32, no. 9, pp. 1–631, 1980.

[18] R. L. Luo, L. S. Cheng, and J. C. Peng, "A new method of determining relationship between permeability and effective overburden pressure for low-permeability reservoirs," *Journal of China University of Petroleum (Edition of Natural Science)*, vol. 2, article 020, 2007.

[19] N. Burdine, "Relative permeability calculations from pore size distribution data," *Journal of Petroleum Technology*, vol. 5, no. 3, pp. 71–78, 1953.

[20] A. T. Corey, "The interrelation between gas and oil relative permeabilities," *Producers Monthly*, vol. 19, no. 1, pp. 38–41, 1954.

[21] I. Fatt, "The effect of overburden pressure on relative permeability," *Journal of Petroleum Technology*, vol. 5, no. 10, pp. 15-16, 1953.

[22] A. Al-Quraishi and M. Khairy, "Pore pressure versus confining pressure and their effect on oil-water relative permeability curves," *Journal of Petroleum Science and Engineering*, vol. 48, no. 1-2, pp. 120–126, 2005.

[23] S. S. Gao, L. Y. Ye, W. Xiong et al., "Seepage mechanism and strategy for development of large and low permeability and tight sandstone gas reservoirs with water content," *Journal of Oil and Gas Technology*, vol. 7, article 020, 2013.

[24] S. Y. Mo, S. L. He, G. Lei, S. H. Gai, and Z. K. Liu, "Effect of the drawdown pressure on the relative permeability in tight gas: A theoretical and experimental study," *Journal of Natural Gas Science and Engineering*, vol. 24, pp. 264–271, 2015.

[25] L. Ye, *Study on Percolation Mechanism and Reservoir Evaluation of Xujiahe Low Permeability Sandstone Gas Reservoirs in Central Sichuan Basin*, Chinese Academy of Science, 2011.

[26] R. Zhang, *Detailed Study on Gas-Water Relative Flow of Tight Gas Sandstone*, Northwest University, 2014.

[27] L. Y. Ye, S. S. Gao, H. Z. Yang et al., "Water Production mechanism and development strategy of tight sandstone gas reservoirs," *Natural Gas Industry*, vol. 35, no. 2, pp. 41–46, 2015.

[28] Y. Liu, Y. Pan, X. Zhen et al., "Influence of rock stress sensitivity in tight gas reservoir on characteristics of gas/water two phase

flows," *Complex Hydrocarbon Reservoirs*, vol. 6, no. 3, pp. 36–39, 2013.

[29] X. Zheng, C. Zhigang, and L. Weichuan, "Gas/water flowing ability influence experimental study of permeability stress sensibility in tight gas reservoir," *Well Logging Technology*, vol. 4, pp. 360–363, 2013.